7. ANKARA INTERNATIONAL AEROSPACE CONFERENCE AIAC-2013-059
11-13 September 2013 - METU, Ankara TURKEY

DEVELOPMENT AND ANALYSIS OF FLAT PLATE IN FLAPPING MOTION USING PIEZOELECTRIC ACTUATORS

Özgür Harputlu[1]and D.Funda Kurtuluş[2]
Middle East Technical University
Ankara, Turkey

ABSTRACT

The purpose of this paper is to design a flapping wing system actuated by piezoelectric materials. The paper includes the selection of piezoelectric actuator and decisions for driving mode as well. The analytical calculations are done using the piezoelectric constitutive relations and material, geometry and configuration properties of the experimental setup. The deflection results are used as inputs to the computational fluid dynamics analysis. Finally, flow field around the beam in flapping motion is solved taking elastic deformation of the beam into consideration.

INTRODUCTION

The technology of unmanned aerial vehicles (UAV) has a rapid improvement and their use is increasing day by day for military and civilian missions. Developments in production technology enable the fabrication of micro aerial vehicles. Flapping wing systems have an important place among UAVs. These vehicles are superior to fixed wing aircrafts with their high maneuverability and hover capability and successfully perform many missions in which the fixed aircrafts are insufficient. Developments in material technology provided the use of smart materials and their integration to the engineering applications. Piezoelectric materials are widely used in aerial vehicle applications, especially in active vibration control. Mechanical and electrical properties are coupled in piezoelectric materials. Piezoelectric materials create mechanical deformation when a voltage is applied across them, or in reverse manner they create electrical charge under mechanical deformation.

Researchers in Harvard University developed a flapping wing micro air vehicle actuated by piezoelectric materials, which can create a sufficient aerodynamic force to lift its own weight [Wood, 2007]. A micro air vehicle with 60mg weight and a 3cm wing span is developed by using laser micromachining production technology. System is driven on 110Hz resonance frequency to achieve maximum tip deflection of piezoelectric actuator. In Figure 1 the developed system and in Figure 2 the piezoelectric bimorph actuator and its motion are shown respectively.

[1] GRA in Department of Aerospace Engineering in Middle East Technical University,
Email: ozgurharputlu@gmail.com
[2] Assoc.Prof.Dr in Department of Aerospace Engineering in Middle East Technical University, Email: funda.kurtulus@gmail.com

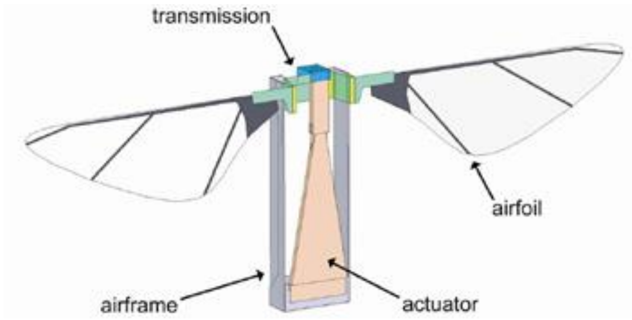

Figure 1: Harvard Microrobotic Fly and its main components [Wood, 2007]

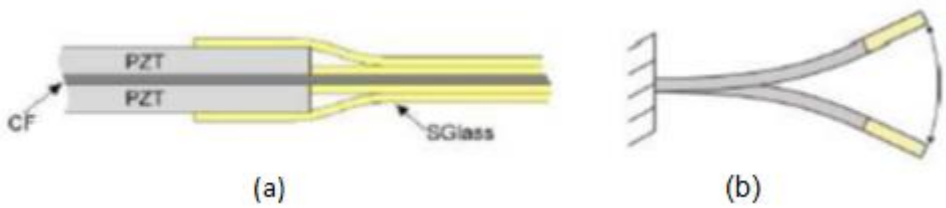

Figure 2: (a) Piezoelectric bimorph actuator used in Harvard Microrobotic Fly
(b) Actuator motion in bending mode [Wood, 2007]

An active flapping wing system with piezoelectric actuators is developed in University of Electro-communications of Japan [Ming et al, 2009]. The active flapping system does not need a mechanical transmission system to amplify the displacement of the actuators and has a resonance frequency of 16Hz. The actuator-wing connection type are observed. In Figure 3, developed wing mechanism and different actuator connection types are shown.

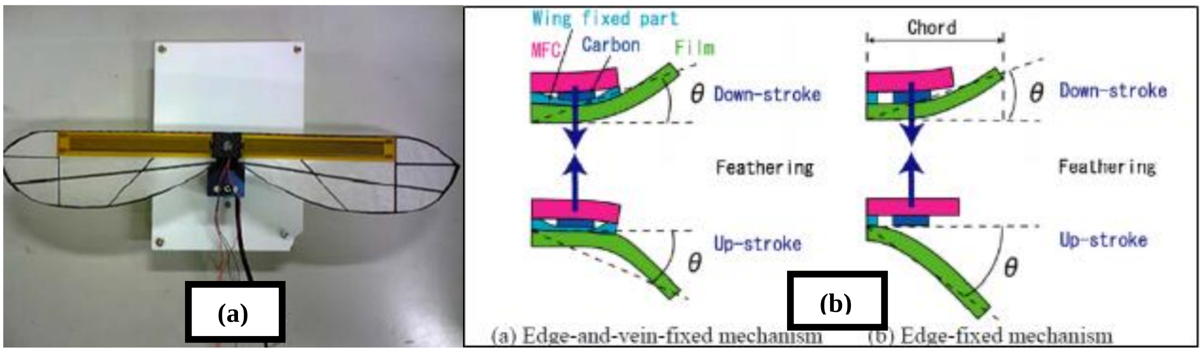

Figure 3: (a) Active flapping wing system (b) Different actuator connection configurations in active flapping system [Ming et al., 2009]

In Konkuk University of Korea lightweight composite piezoceramic actuators (LIPCA) are used to drive flapping wing mechanism with 10Hz resonance frequency [Syafiuddin et al., 2006]. A mechanical amplification is provided by four-bar linkage system. The effects of clap motion and corrugated and smooth wing surfaces on the forces are analyzed. The flapping wing system and four-bar linkage are shown in Figures 4.

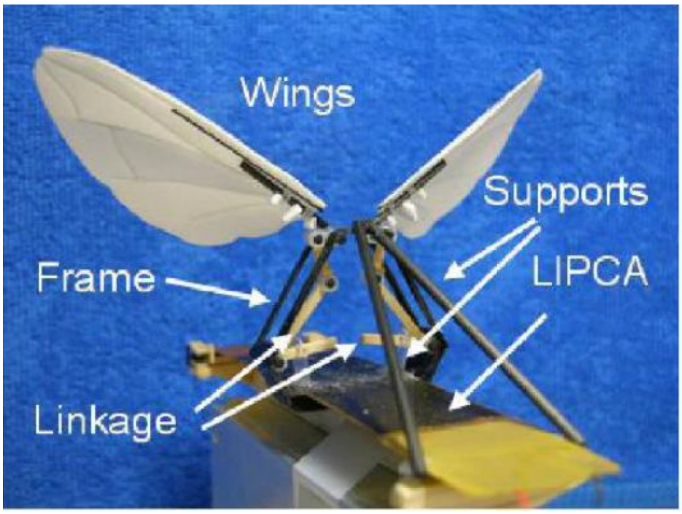

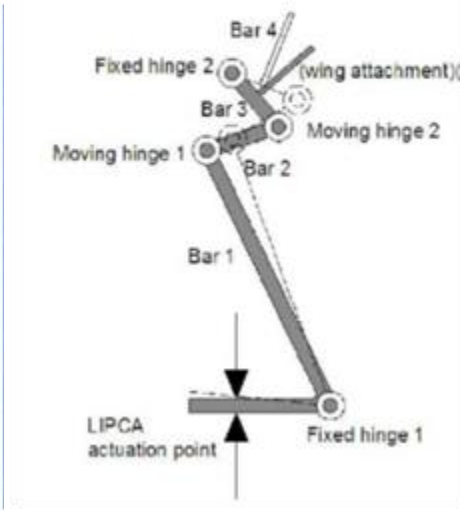

a) LIPCA actuated flapping wing system b) Four-bark linkage mechanism used for mechanical amplification

Figure 4: Flapping wing mechanism with 10Hz resonance frequency [Syafiuddin et al., 2006]

Piezoelectric Actuator Selection

Piezoelectric materials have dipole structures in atomic level. Piezoceramics are solid mixtures of piezo crystallites and initially have randomly oriented dipoles. Piezoceramic materials go under a polarization process to have a surviving polarity. Polarization axis is in the direction of orientation of dipoles. Piezoelectric materials have two main driving modes which are longitudinal and transverse modes. In longitudinal mode piezoelectric materials create force and deflection in the direction of polarization axis. This mode creates small displacement and is generally used in stack actuators. In transverse mode, deflection and force are created out of the polarization axis and generally used to create axial or bending motion. Since the bending motion is desired in the design, the system will be driven in transverse mode. Rectangular piezoceramic (PZT) actuators with dimensions of 70mm x 20mm x 0.5 mm will be used. The actuators will be patched on the top and bottom surfaces of a cantilevered flat plate. The actuators will be driven with the same magnitude but the opposite sign voltages, causing one actuator to contract while the other one expands. Voltage function will have a continuous sinusoidal form and this driving method will result in bending motion on the plate. The longitudinal and transverse modes are shown in Figure 5. Extension and bending motions of the beam by using PZT actuators are shown in Figure 6.

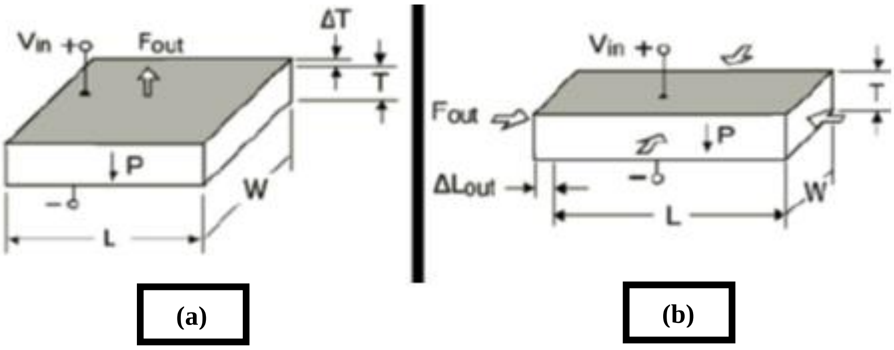

Figure 5: (a) Longitudinal mode (b) Transverse mode of piezoelectric materials [Leo,D.J. 2007]

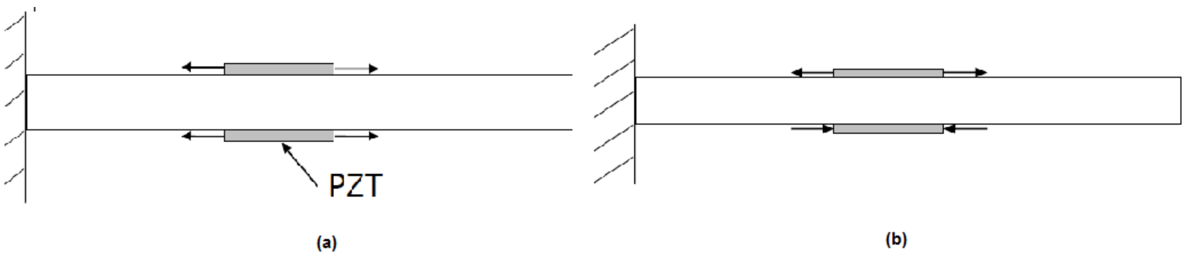

Figure 6: (a) Extension of beam by PZT actuators (b) Bending of beam by PZT actuators

EXPERIMENTAL SETUP

The designed experimental setup consists of an aluminum beam and two piezoelectric actuators. The beam is in cantilevered configuration and piezoelectric actuators are patched on the top and bottom surfaces at the fixed end. A high voltage source, a power amplifier and a function generator are used to drive the actuators. Figure 7 shows the CAD drawing of the experimental setup and the beam configuration. The aluminum beam has dimensions of 150mm length, 20mm width and 1.23 mm thickness and each actuator has 70mm length, 20mm width and 0.5mm thickness. The function generator can generate ± 10 V signal and it is increased by 15 times by the high voltage power amplifier.

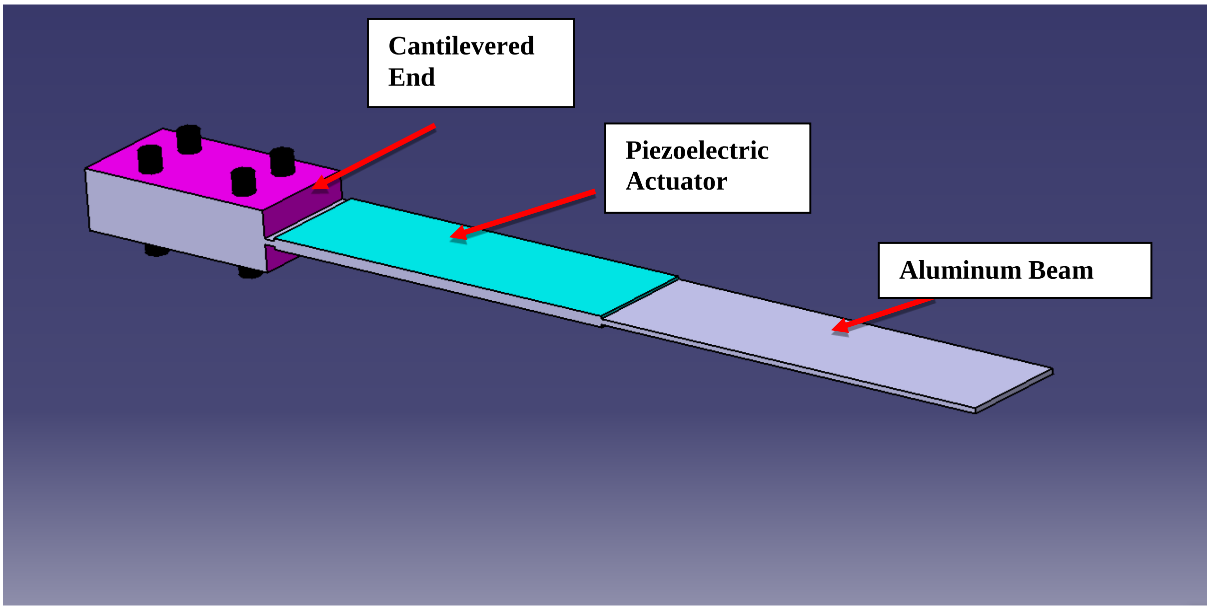

Figure 7: The CAD drawing of the experimental setup and the beam configuration

METHOD

The analytical calculations are performed using the constitutive relations (Eq.1-Eq.4) for linear, orthotropic piezoelectric material operated in 31 mode [Leo, 2007].

$$S_1 = -\frac{1}{Y_1^E} T_1 + d_{13} E_3 \qquad \text{Eq.1}$$

$$S_2 = -\frac{\nu_{21}}{Y_1^E} T_1 + d_{23} E_3 \qquad \text{Eq.2}$$

$$S_3 = -\frac{\nu_{31}}{Y_1^E} T_1 + d_{33} E_3 \qquad \text{Eq.3}$$

$$D_3 = d_{31} T_1 + \varepsilon_{33}^T E_3 \qquad \text{Eq.4}$$

where S_1, S_2, S_3 are normal stress components, d_{13}, d_{23}, d_{33} are piezoelectric strain coefficients and E_3 is the applied electric field. The elastic curve of the beam is obtained by applying the boundary conditions for the cantilevered configuration with the Euler-Bernoulli beam assumption.

$$W(x) = \frac{M}{E_s I_{beam}} \left[\frac{\langle x-x_1 \rangle^2}{2} - \frac{\langle x-x_2 \rangle^2}{2} \right] \quad \text{Eq.5}$$

$$\boldsymbol{M = -E_s \frac{P}{1-P} \frac{2}{3}\, b\, h^2 \mathcal{E}_p} \quad \text{Eq. 6}$$

where x_1 and x_2 denotes the actuator boundaries from the cantilevered end.

The geometric and material property values are used according to the elements in the experimental setup designed. The operating voltage and driving frequency are chosen as ± 150 V and 20Hz respectively depending on the capabilities of the function generator and the power amplifier. The deflections of the different points along the beam longitudinal axis are obtained.

The ANSYS software is used for the numerical analysis of the system. Since the beam goes under an elastic deformation, a coupled analysis between structural and fluid systems is performed. The deflection values for different locations are used as inputs to the structural analysis system. The structural system is linked to the CFX fluid flow analysis system and the flow field around the elastically deformed beam. The section view of mesh generated for the flow field simulation is shown in Figure 8. The mesh for the flow field analysis has 36785 nodes and 197352 cell elements.

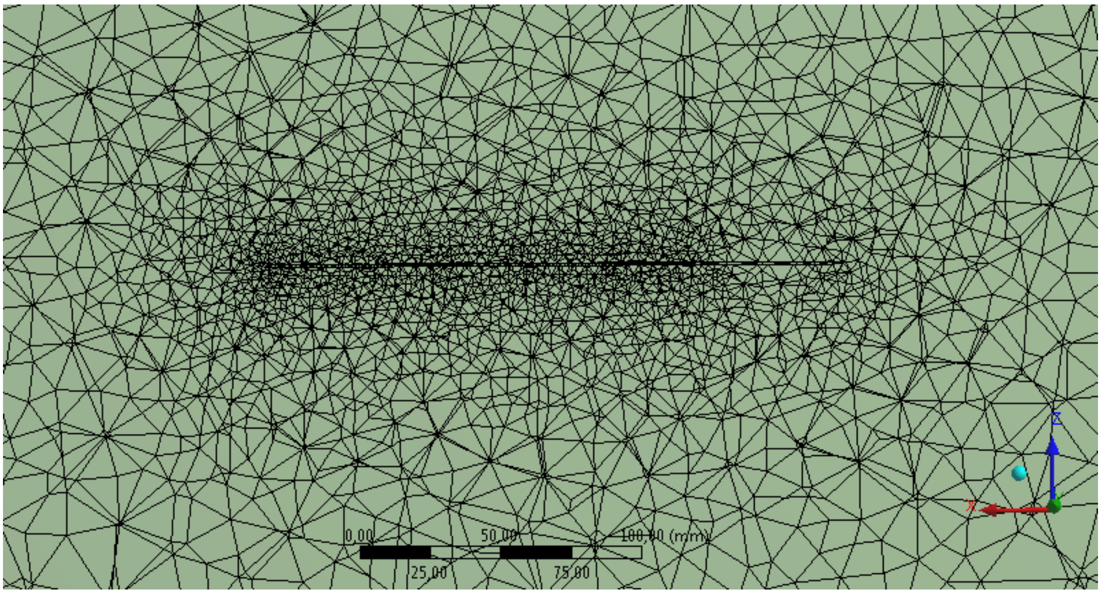

Figure 8: Section View of Mesh for the Fluid Flow System at the Beam Location

RESULTS

The experimental setup is designed for an aluminum beam with elastic modulus of $\mathbf{70\ \boldsymbol{GPa}}$ for the and for the piezoelectric actuator with elastic modulus of $\mathbf{100\ \boldsymbol{GPa}}$. The analytical calculations are performed by using the Eqs 1-6. The piezoelectric strain coefficient of the selected actuator, $\boldsymbol{d_{31}}$, is $\mathbf{185\boldsymbol{x}10^{-12}}\ \boldsymbol{m/V}$. The parameters are inserted into the equation of the elastic curve and the results show that the system can create 14.11 mm tip deflection on the free end due to the bending moment created by two piezoelectric actuators. The elastic curve of the beam has a second order parabolic shape in the actuator boundaries and a constant linear slope after the actuator position within the same time step. The displacement values are calculated for the points at which the input parameters are entered to the numerical simulation. The system is operated by a sinusoidal voltage of ± 150 V with 20 Hz frequency. The displacement vs. time graph for the points with distances of 30, 60, 90,120 and150 mm from the cantilevered end point is shown in Figure 9. The points at which the displacements are inserted are shown in Figure 10.

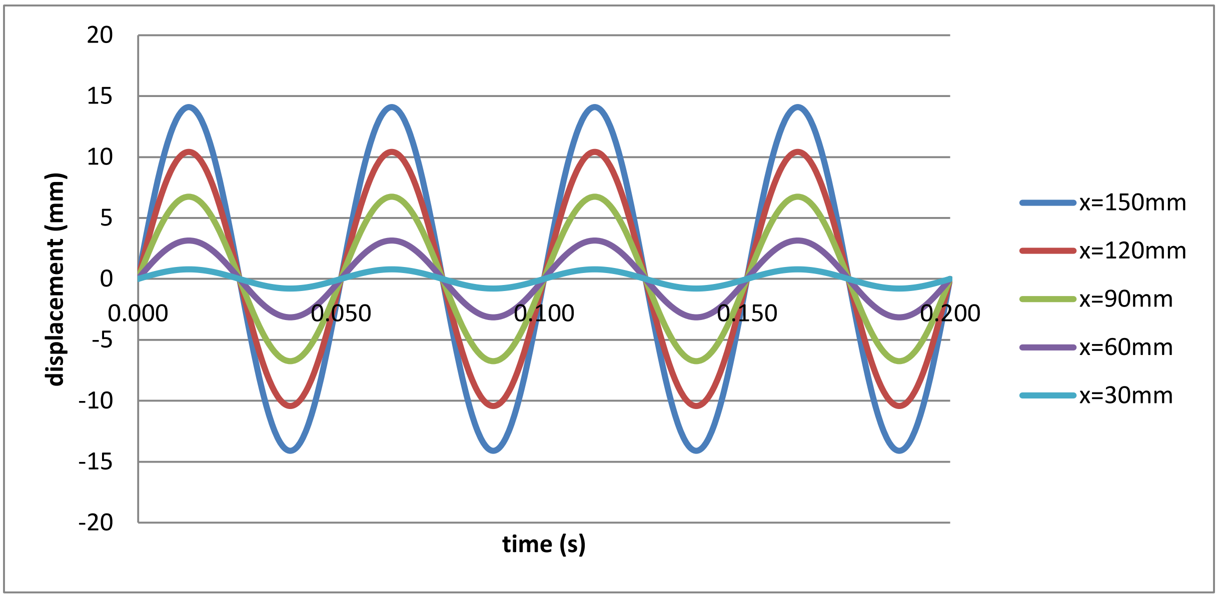

Figure 9: Displacement for the selected points used an input for the numerical analysis

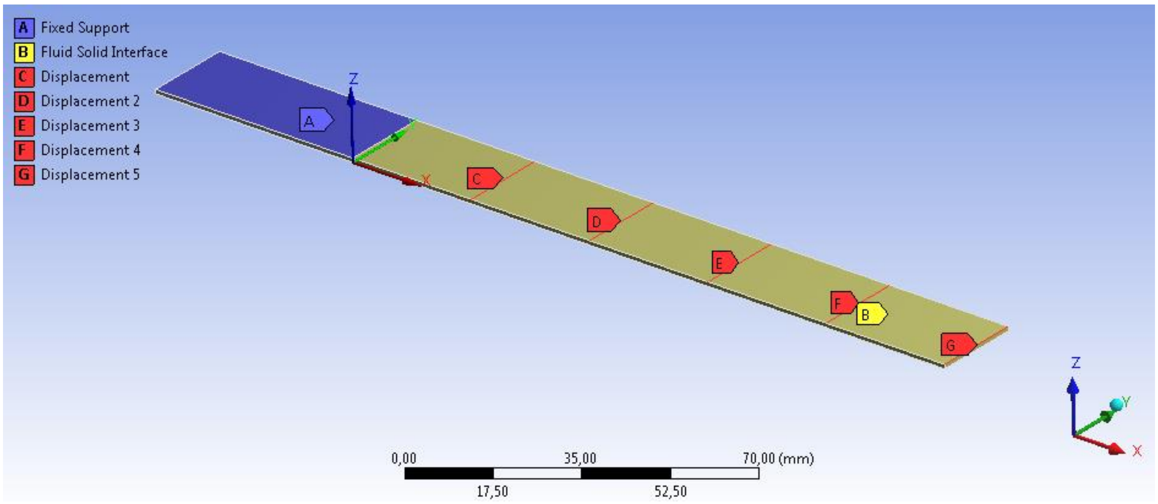

Figure 10: Structural Displacement Input Locations

Section A in Figure 10 represents the fixed part of the beam, which is screwed to a wooden block in the experimental setup to create cantilevered end. Section B shows the part that has an elastic deformation when the actuators are operated and the PZT actuators are located in the 70mm part of section B staring from the cantilevered end.

The numerical simulation is performed using the displacement results obtained from the analytical calculations as inputs. The lift and drag histories of the flapping motion are shown in Figure 11 and Figure 12, respectively.

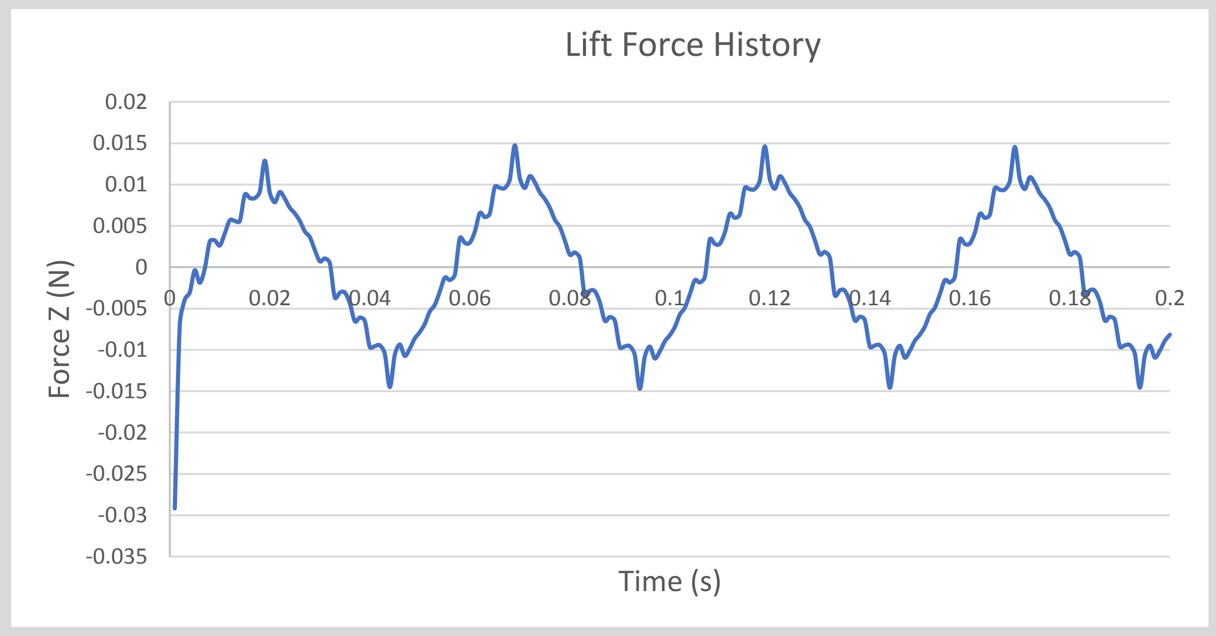

Figure11: Lift Force History

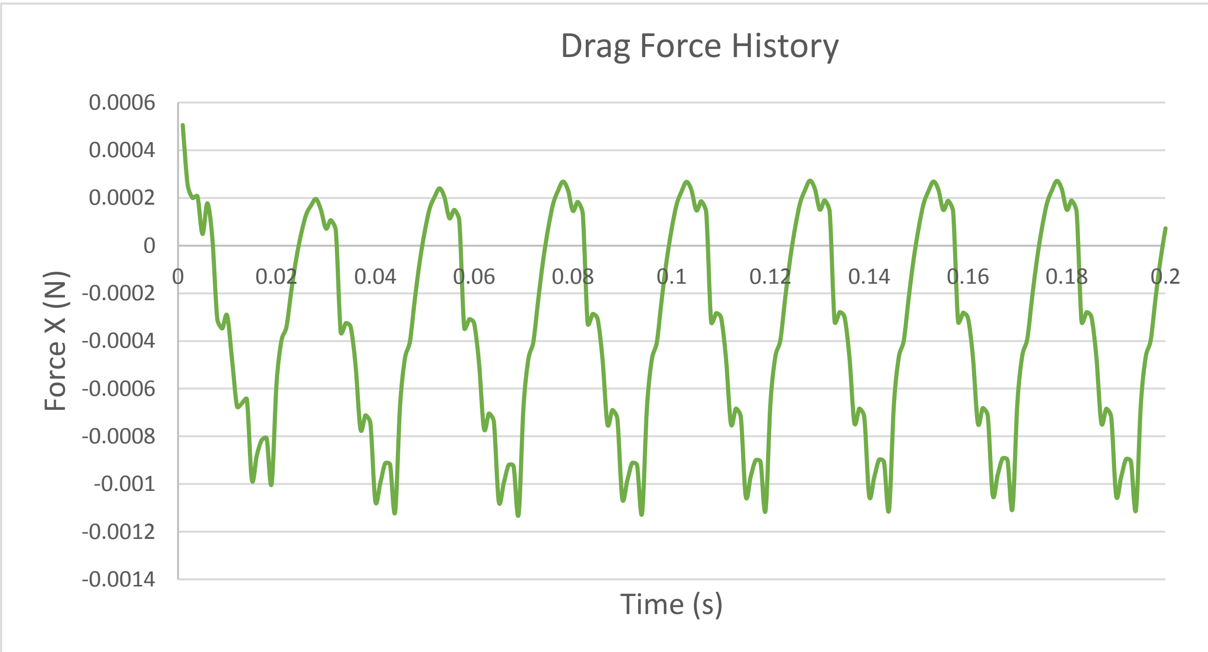

Figure12: Drag Force History

The lift and drag force histories are plotted considering the forces at the interface plate and the time axis corresponds to time steps accumulated. The current analysis has time step of 0.001s and one flapping period is completed at fifty time steps. The lift force is measured in positive z direction and the drag force is measured in negative x direction. The mechanism is shown to generate aerodynamic forces in flapping motion. Since the upstroke and downstroke motions are symmetric, the system does not generate a positive mean lift force, but it generates a mean drag force. Figure 11 shows the pressure contours around the beam and the elastic curve at different time steps. Time steps are chosen so as to show flow field at the initial position, intermediate points in strokes and limits of the up and down stroke motions. The vortex formations at different time steps are shown in Figure 12.

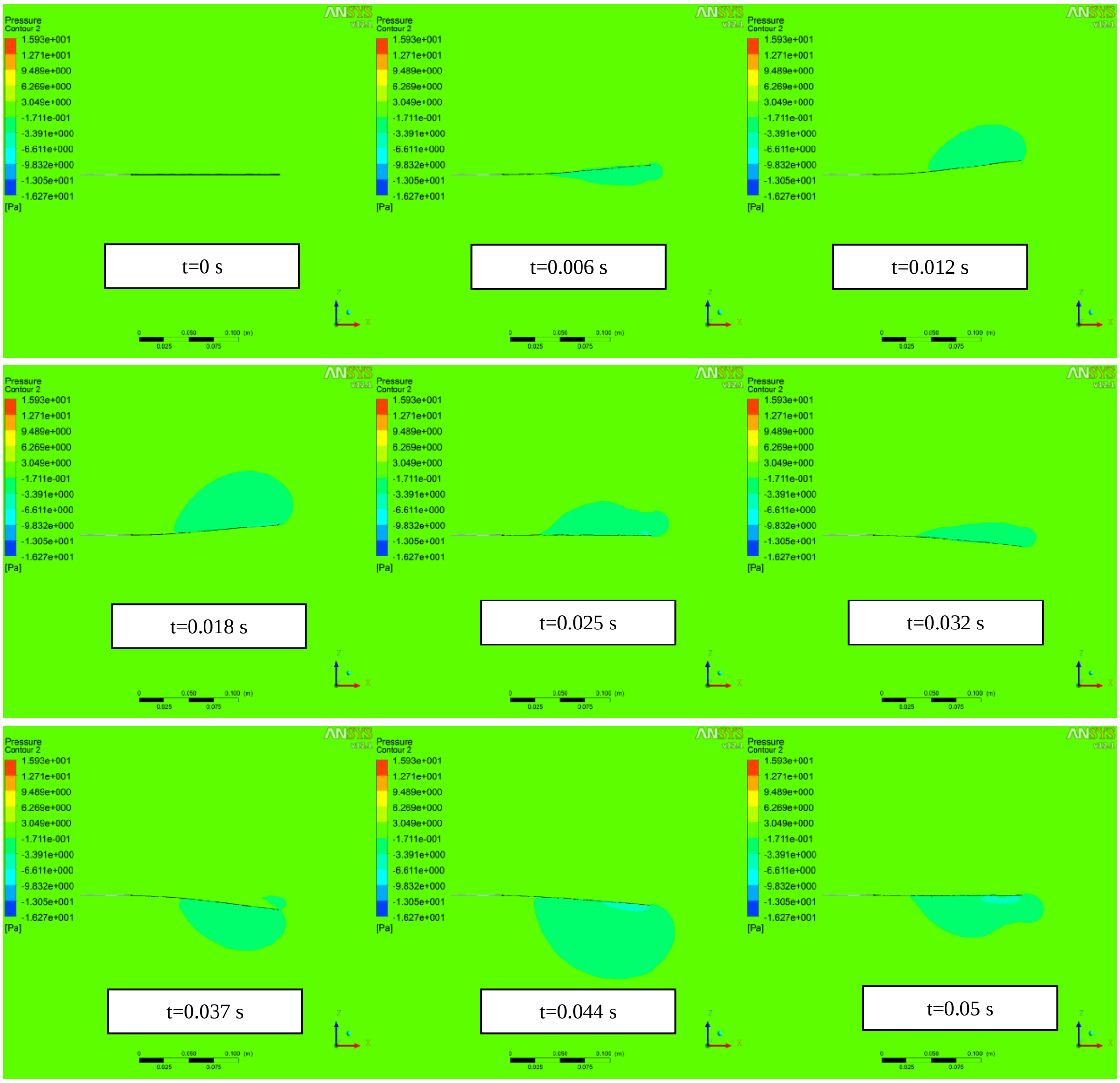

Figure11: Pressure Contours around beam at different time steps with the sinusoidal motion having period of T=0.05 sec at y=0 m

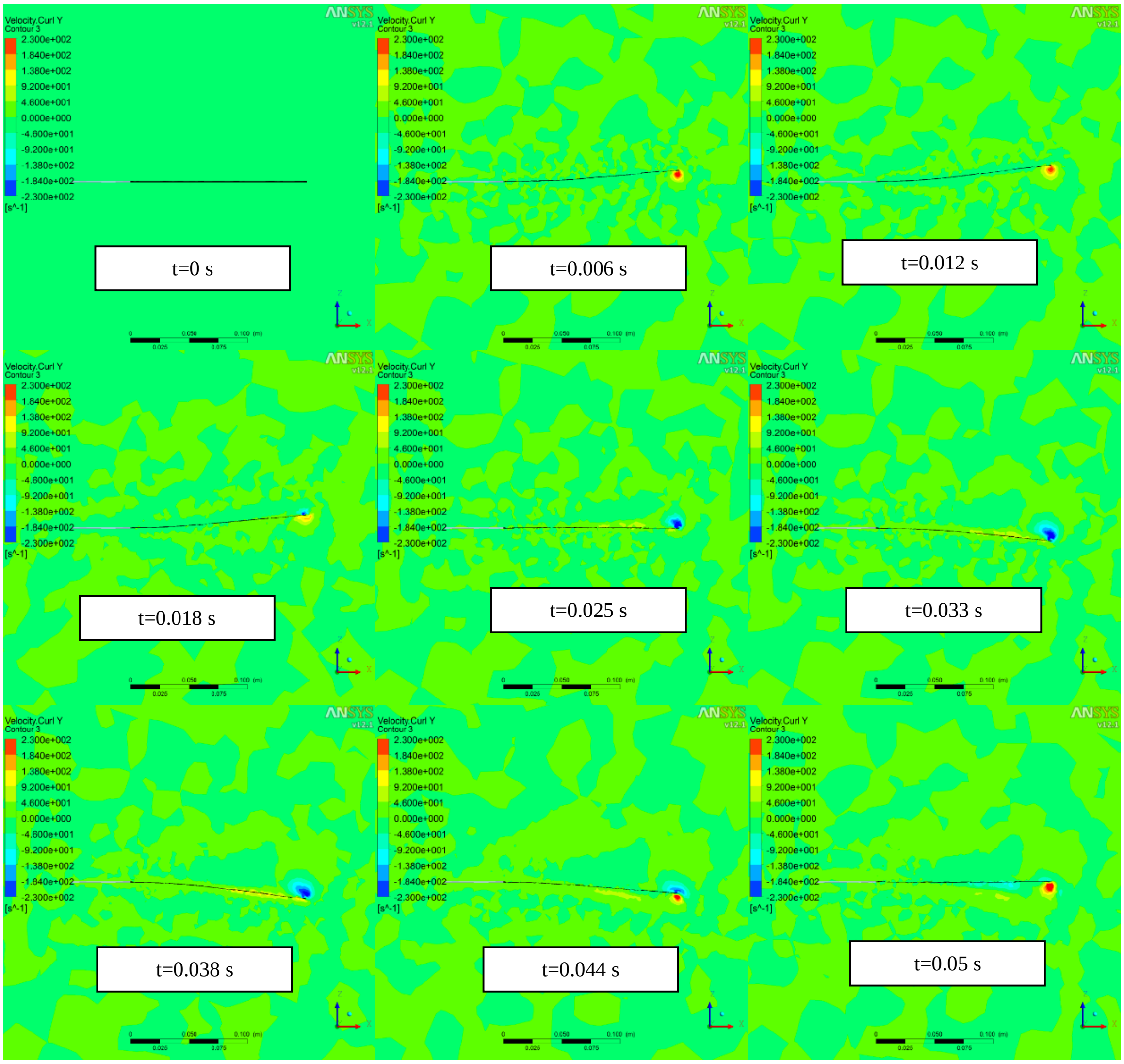

Figure12: Vortex formations at different time steps at y=0 m

The vortex strength is maximum at the free end of the beam deflection of which is the highest absolute value. The upstroke motion creates a positive velocity curl in y direction, whereas the downstroke motion creates a negative velocity curl. The vortex formation change at different y stations is shown in Figure 13. The time step is chosen as 0.012 s, which is close to the end of the first half of the upstroke motion.

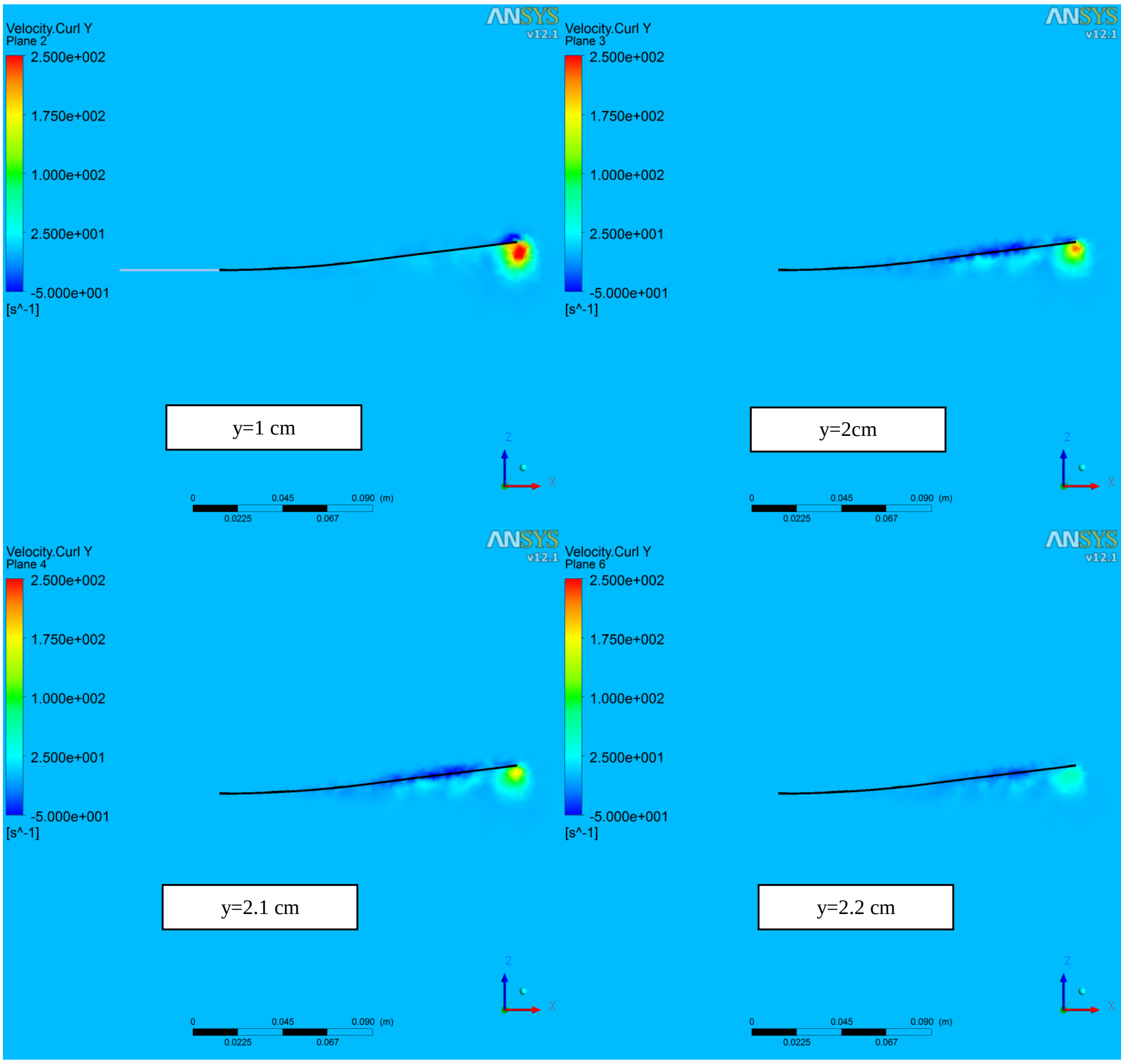

Figure13: Vorticity change in spanwise direction at t= 0.012 sec

The velocity curl is shown be highest at the mid-plane of the beam. The section location at y=0cm and y=2cm refers to beam edges and y=1cm shows the midspan location. The vortex strength at the beam edge is smaller than the center. There is a rapid decrease observed after the plane location passes the beam edge line.

CONCLUSION

In this study flapping system with piezoelectric actuators is analyzed. Piezoelectric actuator is selected concerning the system to be developed and operating mode. The elements of the experimental setup are specified and analytical calculations are performed accordingly to the system specifications. The elastic curve of the beam is obtained and it is used as input to obtain the flow field around the system in flapping motion by using ANSYS software. The piezoelectric actuators can create bending moment on the beam and driving them by continuous square or sinusoidal waves the beam undergoes a flapping motion.

FUTURE WORKS

The current study will continue with the development of the experimental setup. The piezoelectric materials create limited displacement, so an intermediate linkage mechanism can be used to mechanically amplify the displacement created by piezoelectric actuators. The actuators will be driven by high voltage power source and the elastic curve of the beam will be obtained by using high speed camera system. The elastic deformation information will be used as input to the numerical analysis for the flow field. Results of the analytical and experimental studies will be compared.

ACKNOWLEDGEMENT

TÜBA GEBİP Award given to Dr. Kurtuluş is greatly acknowledged (Award No: D.F.K/TÜBA GEBİP/2012-18).

References

Leo, D.J.(2007) *Engineering analysis of smart material systems*, Hoboken, N.J.: Wiley, (2007)

Ming A., Huang,Y. , Fukushima Y., ve Shimojo M.(2009) *Development of an Active Flapping Wing Using Piezoelectric Fiber Composites* , Proceedings of IEEE International Conference on Robotics and Biomimetics

Syaifuddin M., Park H.C., Goo N.S.(2006) *Design and evaluation of a LIPCA-actuated flapping device*, Smart Materials and Structures Vol.15 pp. 1225-1230

Wood R.J.(2007) *Liftoff of a 60mg flapping-wing MAV*, IEEE/RSJ International Conference on Intelligent Robots and Systems, pp.1889-1894